Open access • Posted Content • DOI:10.33774/CHEMRXIV-2021-8CP0Q-V2

Design, Synthesis, and Evaluation of Trivalent PROTACs Having a Functionalization Site with Controlled Orientation — Source link

Yifan Huang, Hiromasa Yokoe, Ai Kaiho-Soma, Kazunori Takahashi ...+4 more authors

Institutions: Hoshi University

Published on: 04 Oct 2021 - ChemRxiv

Topics: Ethylene glycol

Article

Design, Synthesis, and Evaluation of Trivalent PROTACs Having a Functionalization Site with Controlled Orientation

Yifan Huang,[a] Hiromasa Yokoe,[b,d] Ai Kaiho-Soma,[c] Kazunori Takahashi,[b] Yusuke Hirasawa,[b] Hiroshi Morita,[b] Fumiaki Ohtake,[b,c]* Naoki Kanoh[b,d]*

[a] Graduate School of Pharmaceutical Sciences, Hoshi University, 2-4-41 Ebara, Shinagawa-ku, Tokyo 142-8501, JAPAN

[b] School of Pharmacy and Pharmaceutical Sciences, Hoshi University, 2-4-41 Ebara, Shinagawa-ku, Tokyo 142-8501, JAPAN

[c] Institute for Advanced Life Sciences, Hoshi University, 2-4-41 Ebara, Shinagawa-ku, Tokyo 142-8501, JAPAN

[d] Institute of Medicinal Chemistry, Hoshi University, 2-4-41 Ebara, Shinagawa-ku, Tokyo 142-8501, JAPAN

E-mail: f-ohtake@hoshi.ac.jp; n-kanoh@hoshi.ac.jp

Abstract

Trivalent PROTACs having a functionalization site with controlled orientation were designed, synthesized, and evaluated. Based on the X-ray structure of BRD protein degrader MZ1 (**1**) in complex with human VHL and $BRD4^{BD2}$, we expected that the 1,2-disubstituted ethyl group near the JQ-1 moiety in MZ1 (**1**) could be replaced by a planar benzene tether as a platform for further functionalization. To test this hypothesis, we first designed six divalent MZ1 derivatives, **2a-c** and **3a-c**, by combining three variations of substitution patterns on the benzene ring (1,2-, 1,3-, and 1,4-substitution) and two variations in the number of ethylene glycol units (1 or 2). We then tested the synthesized compounds for the BRD4 degradation activity of each. As expected, we found that 1,2D-EG2-MZ1 (**2a**), an MZ1 derivative with 1,2-disubstituted benzene possessing two ethylene glycol units, had an activity profile similar to that of MZ1 (**1**). Based on the structure of **2a**, we then synthesized and evaluated four isomeric trivalent MZ1 derivatives, **15a**-**15d**, having a *tert*-butyl ester unit on the benzene ring as a handle for further functionalization. Among the four isomers, 1,2,5T-EG2-MZ1 (**15c**) retained a level of BRD4 depletion activity similar to that of **2a** without inducing a measurable Hook effect, and its BRD4 depletion kinetics was the same as that of MZ1 (**1**). Other isomers were also shown to retain BRD4 depletion activity. Thus, the trivalent PROTACs we synthesized here may serve as efficient platforms for further applications.

Keywords

Targeted Protein Degradation, Trivalent PROTAC, BRD4, Controlled Orientation, Synthetic Probes, Mode of Action

Main text

Introduction

Targeted protein degradation is an emerging modality for pharmacotherapeutics of human diseases.[1,2] Unlike the traditional small-molecule drugs such as enzyme inhibitors and receptor ligands, protein degraders utilize ubiquitin−proteasome systems, which are major protein degradation mechanisms in mammalian cells. Degraders are intended to bind to both a protein of interest (POI) and a E3 ubiquitin ligase to form their ternary complex and facilitate the polyubiquitination of POI. The resultant ubiquitinated POI is then recognized and degraded by proteasome.

Protein-targeting chimeras, also known as PROTACs, are among the most developed protein degraders so far. This type of degrader is usually composed of three components: a POI ligand, an E3 ligase ligand, and a linker moiety connecting the two. Stable and efficient ternary complex formation is currently believed to be the most important requirement for such bifunctional molecules to be efficient and highly active protein degraders,[3] which are believed to work by hijacking existing ubiquitin−proteasome systems.[1,2] After ternary complex formation, however, the molecular mechanisms by which POI is decorated with ubiquitin chains and delivered to the proteasome are largely unknown. Several regulators, such as p97,[4] TRIP12,[5] UBE2G,[6] and components of the cullin neddylation cycle,[7] have been reported to promote targeted protein degradation. This suggests a possibility that additional as-yet-unknown factors may play important roles in PROTAC-mediated

protein degradation. In addition, few studies have been carried out to understand the spatiotemporal dynamics and subcellular localization of PROTAC-mediated ternary complexes[8,9] and their components in cells. Thus, PROTAC probes for detecting as-yet-unknown components of PROTAC-induced protein degradation and those for localization analyses would be useful not only for understanding the mechanism underlying the forced degradation of neo-substrates but also for developing highly active PROTACs.

Recently, trivalent PROTACs have been gaining increasing attention because an additional third site can be used to integrate additional functions on PROTACs. For example, Kim *et al*.[10] and Ciulli *et al*.[11] introduced two POI ligands into a PROTAC via a flexible linker to enhance binding valency and cooperativity, generating two-headed ER-ligand−based PROTAC and SIM1, respectively (Figure 1). Especially, trivalent PROTAC SIM1,[11] which is based on BRD4 degrader MZ1 (**1**)[12,13] and a bivalent BRD4 binder (not shown),[14] accomplished low picomolar degradation of BRD proteins. Dragovich *et al*.[15,16] developed potent antibody−PROTAC conjugates (ADC) such as DAR6 STEAP-1 ADC, in which a BRD4-targeting PROTAC was integrated on a cancer-targeting antibody via a cleavable linker. Liu *et al*.[17] also developed cancer-selective PROTACs, exemplified by folate-ARV-771, by conjugating a folate group to a VHL ligand of ARV-771 in order to achieve selective targeted degradation of POIs in cancer cells versus noncancerous normal cells.

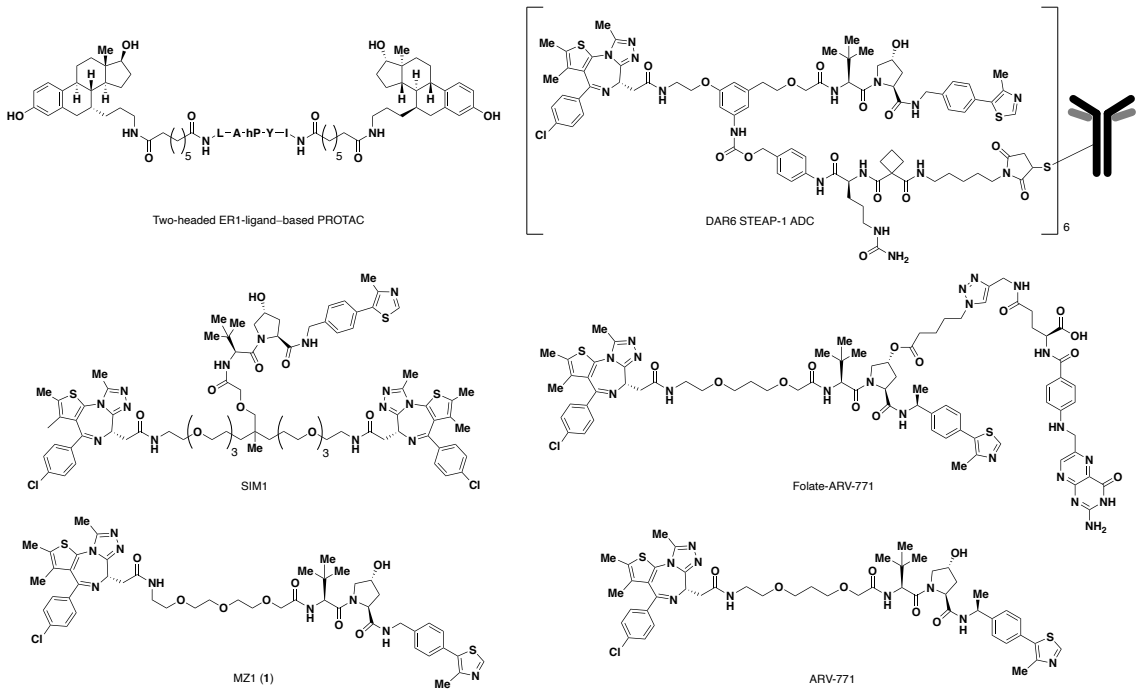

Figure 1. Trivalent and divalent PROTACs. hP = hydroxyproline.

We envisioned that the third site introduced in PROTACs would be used not only to achieve higher activity and selectivity, but also to generate probe molecules for mode-of-action studies by conjugating reporter functional groups such as fluorophores, turn-on fluorescent reagents,[18] and ligand-directed affinity reagents.[19] Moreover, if we could introduce an affinity labeling reagent in a PROTAC with controlled orientation, the resultant molecules would be intelligent PROTAC probes that could be used to analyze the fate of ternary complex components in a spatiotemporal manner (vide infra).

We herein present the design, synthesis, and evaluation of trivalent PROTACs having a functionalization site with controlled orientation. Our trivalent PROTACs each consist of a VHL ligand AHPC, a BRD4 ligand JQ-1 carboxylic acid, and a handle for further functionalization, each of

which is tethered via a trisubstituted benzene ring having a different substitution pattern. The resultant trivalent PROTACs retained BRD4 degradation activity, and the BRD4 degradation time course of the most potent one was comparable to that of MZ1 (**1**). These trivalent PROTAC molecules would be good and multipotent platforms for further probe development.

Results and Discussion

Our trivalent PROTAC design is based on the reported crystal structure[13] of MZ1 (**1**) in complex with a human VHL protein and a BRD4 bromodomain 2 protein ($BRD4^{BD2}$) (Figure 2A and 2B). In the X-ray structure, MZ1 (**1**) folds into itself to allow the formation of specific intermolecular interactions in the ternary complex and of the PEG linker moiety near the JQ-1 moiety exposed to solvent (Figure 2A, yellow dashed ellipse). We analyzed the dihedral angles of the PEG linker of this region and found one (N-C-C-O) that was close to zero (17.6°) (Figure 2B). Thus, we envisioned that a planar 1,2,x-trisubstituted benzene ring (x=3~6), instead of a 1,2-disubstituted ethyl group, could be inserted here as a platform for functionalization (Figure 2C). Four isomers are possible for the 1,2,x-trisubstituted benzene; thus, they would be useful platforms for probe molecules if their BRD4 degradation activity and BRD4 depletion kinetics were comparable to those of MZ1 (**1**). For example, if a nucleophile-reactive affinity labeling functional group was present near the nucleophilic amino acid residue of a ternary complex component, the transferred label could be used to follow the time-dependent

localization of the component during and after the ternary complex formation (Figure 2D). Moreover, the affinity labeling functional group oriented toward the outside of the complex could be used to discover as-yet-unknown factors of PROTAC-induced protein degradation.

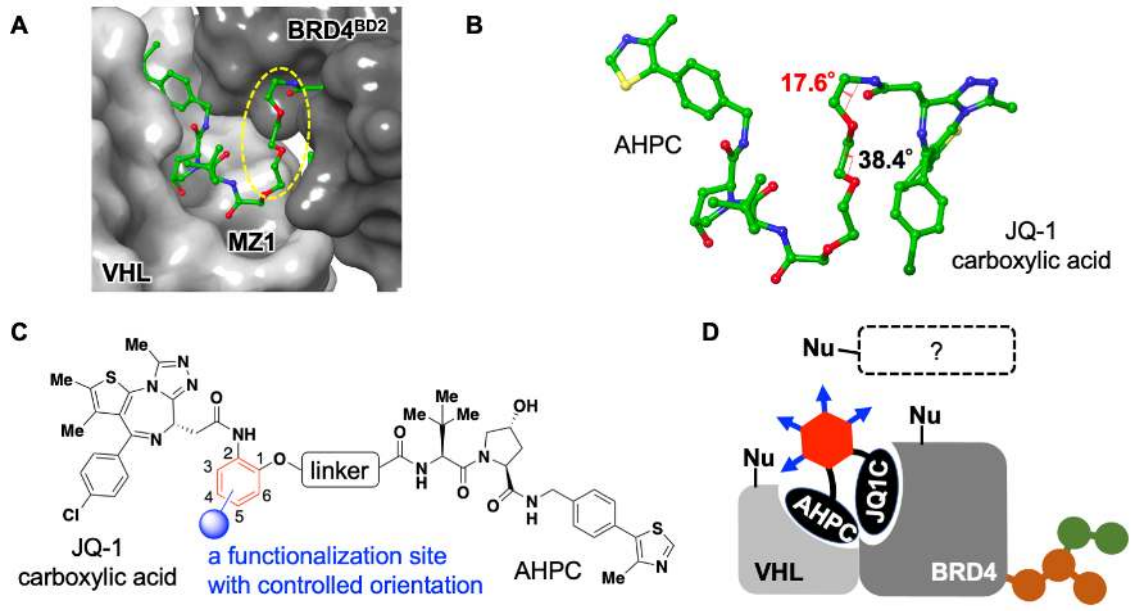

Figure 2. Design of trivalent PROTACs having a functionalization site with controlled orientation. (A) Crystal structure of the VHL:MZ1:BRD4^{BD2} ternary complex (PDB ID 5T35) visualized by using Maestro software (Schrödinger, LLC). (B) Conformation of MZ1 in the ternary complex. Dihedral angles of the PEG linker moiety near the JQ-1. (C) Design of trivalent PROTACs. (D) The designed PROTACs could be used not only to follow the time-dependent localization of the ternary component during and after ternary complex formation, but also to discover as-yet-unknown factors of PROTAC-induced protein degradation.

To validate the effect of the inserted benzene ring and whether the orientations of the VHL and BRD4 ligands and the length of the linker connecting them are optimal, we first synthesized six divalent PROTACs (**2a-c** and **3a-c**) combining three variations of substitution patterns (1,2-, 1,3-, and 1,4-substitution) on the benzene ring and two variations in the number of ethylene glycol units (1 or 2) (Scheme 1). Divalent PROTACs **2a**, **2b**, and **2c**,[20] which have *ortho*-, *meta*-, and *para*-substituted benzenes, respectively, each possess two ethylene glycol units, as in MZ1 (**1**), while the series of PROTACs **3a**, **3b**,[20] and **3c** each have one unit (Scheme 1).

The synthesis of divalent PROTACs **2a-c** was commenced with nucleophilic aromatic substitution (S_NAr) reactions of commercially available *o*-, *m*-, and *p*-fluoronitrobenzene (**4a-c**) with diethylene glycol to afford alcohols **5a-c** in 44-62% yields (Scheme 1A). Introduction of a C2 carboxylic acid unit by bromoacetic acid gave carboxylic acids **6a-c** in 14-48% yields. Coupling with (*S,R,S*)-AHPC (**7**)[21] using HATU,[22] followed by the reduction of the nitro group and a second coupling with JQ-1 carboxylic acid (**10**), afforded the desired divalent PROTACs **2a-c** in 59-68% yields in 3 steps.[20] For the synthesis of truncated divalent PROTACs **3a-c**, alcohols **5a-c** were utilized as starting materials (Scheme 1B): they were oxidized under one-pot oxidation conditions using a catalytic amount of AZADO oxoammonium salt (**11**)[23] to afford carboxylic acids **12a-c** in 61-86% yields. Thereafter, the same 3-step protocol[20] for the synthesis of divalent PROTACs **2a-c** was applied to carboxylic acids **12a-c** to give truncated divalent PROTACs **3a-c** in 23-84% yields in 3 steps.

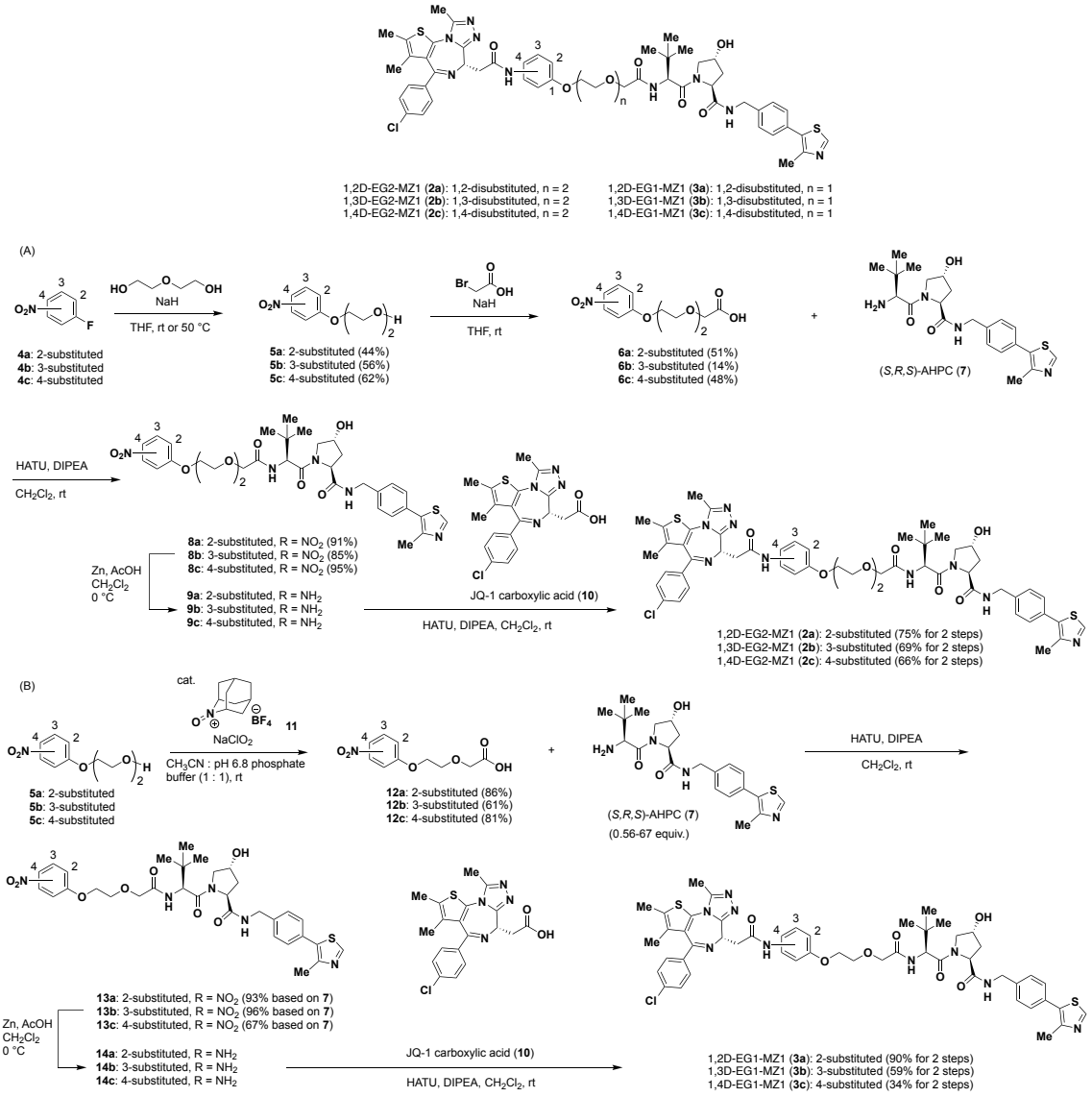

Scheme 1. Synthesis of divalent PROTACs **2a-c** and **3a-c**.

The BRD4 degradation activity of divalent PROTACs **2a-c** and **3a-c** was evaluated by using MZ1 (**1**) as a positive control (Figure 3). To validate the dose-dependent intracellular activity of the synthetic

divalent PROTACs, HT1080 cells were treated with various concentrations of PROTACs, and protein levels of BRD4 were evaluated by Western blotting (Figure 3A). All the compounds showed concentration dependent BRD4 depletion activity. Among them, 1,2D-EG2-MZ1 (**2a**) showed the most potent activity and the smallest Hook effect, although the effective concentration of **2a** was one order higher than that of MZ1 (**1**). We then examined the time-dependent cellular activity of divalent PROTACs **2a-c** and **3a-c** using the optimal concentration of each compound determined from the results of Figure 3A (Figure 3B). The depletion kinetics of 1,2D-EG2-MZ1 (**2a**), 1,3D-EG2-MZ1 (**2b**), 1,3D-EG1-MZ1 (**3b**), and 1,4D-EG1-MZ1 (**3c**) were found to be similar to that of MZ1 (**1**) (Figure 3C). Therefore, we confirmed that 1,2D-EG2-MZ1 (**2a**) was suitable for further trivalent PROTAC development.

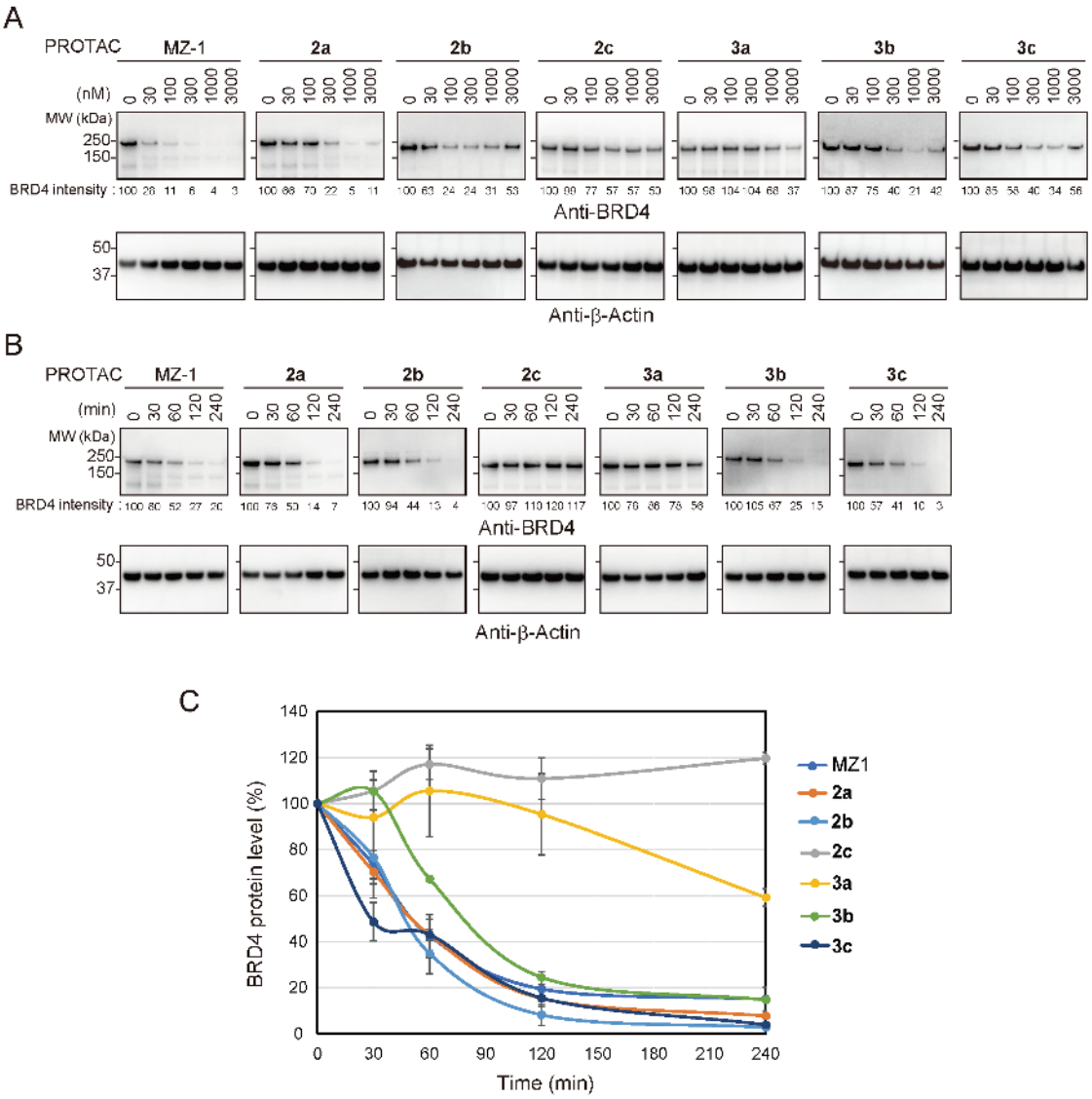

Figure 3. Concentration- and time-dependent degradation of BRD4 induced by divalent PROTACs **2a-c** and **3a-c**. (A) HT1080 cells were treated with different concentrations of **2a-c** and **3a-c** for 2 h. The whole cell lysates were subjected to Western blotting using the indicated antibodies. The band intensities of anti-BRD4 blots are shown below the gel images. (B) Time-course analysis of BRD4 degradation using HT1080 cells treated with either MZ1 (100 nM), **2a** (1000 nM), **2b** (300 nM), **2c** (3000 nM), **3a** (3000 nM), **3b** (1000 nM), or **3c** (1000 nM). (C) Band intensities of anti-BRD4 blots

in (B) (mean +/- S.D., two biological replicates).

Then, trivalent PROTACs **14a-d**, each having a functionalization site with controlled orientation, were designed and synthesized based on 1,2D-EG2-MZ1 (**2a**) (Scheme 2). We chose a *tert*-butyl ester unit as a handle for further functionalization on the benzene tether because acid-promoted deprotection of *tert*-butyl ester and carboxylic acid-based functionalization are well known. In addition, we used the bulkiness of the *tert*-butyl group to examine whether the third site would accept a variety of functional groups.

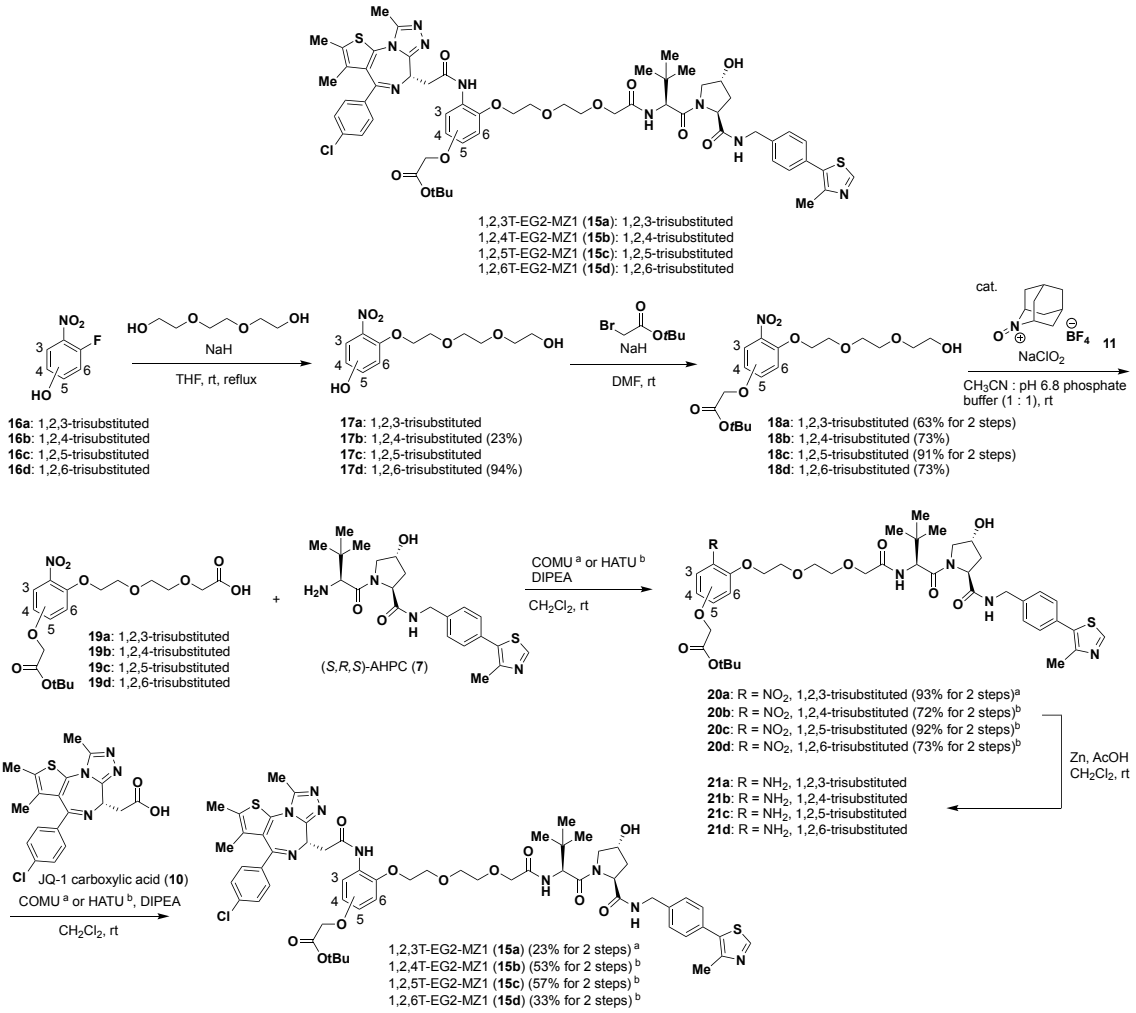

Scheme 2. Synthesis of trivalent PROTACs **15a-d**, each having a functionalization site with controlled orientation.

The trivalent PROTACs **15a-d** were synthesized based on the same strategy used in Scheme 1. Starting from fluoronitrophenols **16a-d**, S_NAr reaction using triethylene glycol followed by phenolic OH-selective Williamson etherification using *tert*-butyl bromoacetic acid gave alcohols **18a-d** (Scheme 2). One-pot oxidation by using a catalytic amount of AZADO oxoammonium salt (**11**)[23] cleanly converted

alcohols **18a-d** to the corresponding carboxylic acids **19a-d**, which in turn were coupled with (*S*,*R*,*S*)-AHPC (**7**) to afford the conjugates **20a-d** in good overall yields. Note that, for the oxidation of alcohols **18a-d**, other conditions, such as PDC oxidation in DMF, did not work, and only the AZADO oxoammonium salt-catalyzed NaOCl-free one-pot oxidation[23] gave the desired products. Finally, reduction of the nitro group of **20a-d** and coupling of the resulting substituted anilines **21a-d** with JQ-1 carboxylic acid (**10**) gave the desired trivalent PROTACs **15a-d**. It should also be noted that HATU-mediated coupling of 1,2,3-trisubstituted aniline **21a** with **10** did not proceed well even using a higher temperature (55 °C in 1,2-dichloroethane), possibly because of the double *ortho*-substitution of the reaction center; thus, the more effective coupling agent COMU[24] was used in this case.

The dose-dependent BRD4 degradation activity of trivalent PROTACs **15a-d** was evaluated (Figure 4). Among the four trivalent PROTACs, 1,2,5T-EG2-MZ1 (**15c**) and 1,2,6T-EG2-MZ1 (**15d**) retained levels of activity similar to that of 1,2D-EG2-MZ1 (**2a**). In addition, 1,2,5T-EG2-MZ1 (**15c**) did not induce a measurable Hook effect up to a concentration of 3 μM. We then evaluated the BRD4 depletion kinetics of **15c** along with MZ1. We found that the depletion kinetics of **15c** was similar to that of MZ1 (**1**) (Figure 4B and 4C), with estimated half-lives (t ½) of BRD4 of 27 min and 36 min, respectively. These results indicated that the third functionalization site introduced in **15c** did not affect ternary complex formation or the following cellular events, suggesting the usability of this

functionalization site to synthesize probes for the analysis of the spatiotemporal dynamics and subcellular localization of PROTACs.

Although a loss of activity and/or a Hook effect were observed for trivalent PROTACs **15a**, **15b**, and **15d**, these compounds each retain a certain degree of BRD4-degradation activity and therefore possess a possibility for further applications.

Taken together, the results indicate that the trivalent PROTACs we synthesized in this study provide platforms to introduce functional moieties into the original compound, MZ1 (**1**). This strategy can be used to synthesize probes for the mode-of-action analysis by conjugation with a fluorescent molecule. Specifically, the third site introduced in each of **15a**, **15c**, and **15d** points toward nucleophilic amino acids in $Brd4^{BD2}$, Tyr98 of VHL, and Glu94 of VHL, respectively (Figure S1). Therefore, after conjugation with a proximity-driven and site-specific affinity reagent, such trivalent PROTACs may serve as efficient tools for analyzing the localization of each component during and after ternary complex formation. In addition, these trivalent PROTACs can be used as platforms for discovering as-yet-unknown factors of PROTAC-induced protein degradation by changing the length of the tether connecting the trisubstituted benzene with the affinity reagent.

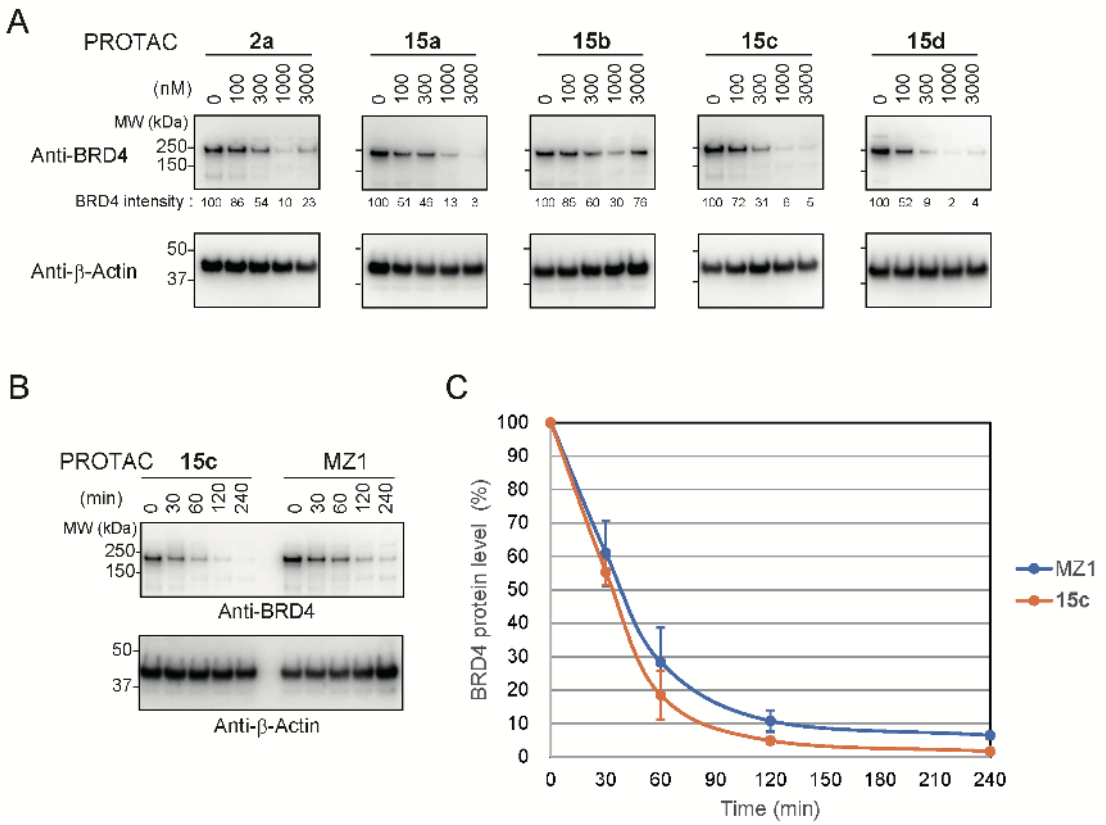

Figure 4. Concentration- and time-dependent degradation of BRD4 induced by trivalent PROTACs **15a-d**. (A) HT1080 cells treated with different concentrations of the indicated PROTACs for 2 h. Degradation of BRD4 was analyzed by Western blotting. (B) Time-course analysis of BRD4 degradation using HT1080 cells treated with either MZ1 (100 nM) or **15c** (1000 nM). (C) Band intensities of anti-BRD4 blots in (B) (mean +/- S.D., three biological replicates).

Conclusion

We designed, synthesized, and evaluated trivalent PROTACs that each had a functionalization site with a controlled orientation. Based on the reported structure of MZ1 (**1**) in complex with human VHL

and $BRD4^{BD2}$, we synthesized and evaluated trivalent PROTACs that each had a *tert*-butyl ester unit on the benzene ring as a handle for further functionalization. Among the compounds synthesized, 1,2,5T-EG2-MZ1 (**15c**) possessed a level of BRD4 depletion activity similar to that of **2a** without inducing a measurable Hook effect up to a concentration of 3 μM, and its BRD4 depletion kinetics was the same as that of MZ1 (**1**). Other isomers were also shown to retain BRD4 depletion activity, indicating the possibility of further applications. We are currently working on the synthesis and evaluation of MZ1 probes based on **15c** to elucidate the cellular localization and fate of the MZ1-induced ternary complex and its components. Finally, although only MZ1-based trivalent PROTACs were developed in this study, the concept of trivalent PROTACs that each have a functionalization site with controlled orientation can be applied to other PROTACs, which will be reported in due course.

Experimental Procedures

General information

All reactions were carried out under an argon atmosphere with dehydrated solvents under anhydrous conditions unless otherwise noted. Reagents were obtained from commercial suppliers unless otherwise noted. All the heated reactions were carried out by using an oil bath. Reactions were monitored by thin-layer chromatography (TLC) carried out on Silica gel 70 F254 glass plates (Wako; 0.25 mm thickness) with visualization by UV light (254 nm) or by staining with *p*-anisaldehyde or

phosphomolybdic acid. Column chromatography was performed on Chromatorex PSQ 100B (Fuji Silysia; spherical, neutral, 100 μm). Preparative thin-layer chromatography (PTLC) was performed on PLC glass plate silica gel F254 (Merck; 1 mm thickness). High-performance liquid chromatography (HPLC) was performed on a JASCO PU-2089 Plus quaternary gradient pump with a JASCO UV-2075 Plus Intelligent UV/VIS detector using a Kinetex 5u C18 100A AXIA column (5 μm, 250 mm × 21.2 mm). The flow rate for HPLC was 8.0 mL/min with 70% MeCN/H_2O. UV detection was performed at 366 nm.

^1H NMR (400 and 600 MHz) and $^{13}C\{^1H\}$ NMR spectra (100 and 150 MHz) were recorded on Bruker AV III 400 and JEOL JNM-ECA-600 spectrometers, respectively. For ^1H NMR spectra, chemical shifts (δ) are given from TMS (0.00 ppm) or $CHCl_3$ (7.26 ppm) in $CDCl_3$. For $^{13}C\{^1H\}$ NMR spectra, chemical shifts (δ) are given from $CDCl_3$ (77.0 ppm) as internal standards. The following abbreviations were used to describe the multiplicities: s = singlet, d = doublet, t = triplet, q = quartet, quin = quintet, sept = septet, dd = double doublet, dt = double triplet, ddt = double double triplet, tt = triple triplet, td = triple doublet, qd = quartet of doublet, m = multiplet, br = broad. ESI mass spectra were recorded on a JEOL JMS-T100LP with a time-of-flight mass analyzer.

Synthesis of divalent and trivalent PROTACs 2a-c, 3a-c, and 15a-d

Synthesis and characterization data of **8a-c**, **13a-c**, and **20a-d** are described in the Supporting

Information. For the synthesis of **2a-c**, **3a-c,** and **15a-d**, each of precursor **8a-c**, **13a-c**, and **20a-d** was treated with Zn powder (40 equiv.) and AcOH (10 equiv.) in CH_2Cl_2 (substrate concentration: 60 mM) at room temperature for 3-24 h. The mixture was filtered and concentrated *in vacuo*. To the crude product were added CH_2Cl_2 (substrate concentration: 60 mM), JQ-1 carboxylic acid (1.0 equiv.), DIPEA (2.0-8.8 equiv.), and coupling agent (HATU or COMU, 1.0-3.0 equiv.) at room temperature. After stirred for 18-24 h, the mixture was concentrated in *vacuo*. The crude material was purified by silica gel column chromatography, PTLC and/or HPLC to give divalent and trivalent PROTAC.

1,2D-EG2-MZ1 (**2a**): purified by silica gel column chromatography (1–5% MeOH/$CHCl_3$) followed by PTLC (5% MeOH/$CHCl_3$); Yield 75% from **8a**; ^{1}H NMR (600 MHz, $CDCl_3$) δ 8.80 (1H, s), 8.68 (1H, s), 8.29 (1H, dd, *J* = 7.9, 1.4 Hz), 7.29–7.40 (10H, m), 7.20 (1H, s), 7.00 (1H, td, *J* = 7.7, 1.4 Hz), 6.95 (1H, td, *J* = 7.7, 1.3 Hz), 6.90 (1H, dd, *J* = 8.1, 1.2 Hz), 4.69–4.71 (2H, m), 4.56 (1H, d, *J* = 8.9 Hz), 4.52 (1H, dd, *J* = 15.1, 6.9 Hz), 4.47 (1H, br s), 4.25 (2H, m), 4.18–4.21 (1H, m), 4.11 (1H, d, *J* = 15.8 Hz), 4.06 (1H, d, *J* = 15.8 Hz), 3.90 (2H, dd, *J* = 9.1, 3.6 Hz), 3.71–3.78 (5H, m), 3.58–3.68 (3H, m), 2.65 (3H, s), 2.50 (3H, s), 2.48-2.52 (1H, m), 2.40 (3H, s), 2.08 (1H, dd, *J* = 13.2 and 8.1 Hz), 1.67 (3H, s), 0.93 (9H, s); ^{13}C{^{1}H} NMR (150 MHz, $CDCl_3$) δ 171.26, 170.88, 170.42, 168.98, 163.93, 155.60, 150.22, 149.88, 148.39, 147.66, 138.18, 136.71, 136.59, 132.01, 131.61, 131.00, 130.82, 130.76, 130.52, 129.93 (2), 129.39 (2), 128.64 (2), 128.49, 128.04 (2), 123.95, 121.60, 120.78, 112.61, 70.90, 70.80, 70.37, 70.07, 69.46, 68.71, 58.43, 56.96, 56.73, 54.15, 43.10, 40.00, 36.01, 35.25, 26.36

(3), 16.04, 14.42, 13.09, 11.79; HRMS (ESI) *m/z*: $[M + Na]^+$ Calcd for $C_{53}H_{60}ClN_9NaO_8S_2$ 1072.3593; Found 1072.3621.

1,3D-EG2-MZ1 (**2b**): purified by silica gel column chromatography (1–5% MeOH/$CHCl_3$) followed by PTLC (5% MeOH/$CHCl_3$); Yield 69% from **8b**; ^1H NMR (600 MHz, $CDCl_3$) δ 9.35 (1H, brs), 8.67 (1H, s), 7.44 (1H, m), 7.32–7.38 (4H, m), 7.31 (4H, m), 7.24–7.28 (1H, m), 7.15 (1H, t, *J* = 1.8 Hz), 6.64 (1H, dd, *J* = 2.4, 9.0 Hz), 4.79 (1H, t, *J* = 8.1 Hz), 4.68 (1H, t, *J* = 6.9 Hz), 4.57 (1H, d, *J* = 8.6 Hz), 4.51–4.53 (2H, m), 4.48 (1H, d, *J* = 6.6 Hz), 4.42-4.48 (1H, m), 4.12–4.20 (4H, m), 4.03 (1H, d, *J* = 15.8 Hz), 3.97 (1H, d, *J* = 15.8 Hz), 3.83–3.86 (1H, m), 3.77 (1H, dt, *J* = 11.3, 4.5 Hz), 3.57-3.71 (7H, m), 2.65 (3H, s), 2.48 (3H, s), 2.39–2.44 (1H, m), 2.40 (3H, s), 2.19 (1H, dd, *J* = 13.2, 7.7 Hz), 1.66 (3H, s), 0.99 (9H, s); $^{13}C\{^1H\}$ NMR (150 MHz, $CDCl_3$) δ 171.27, 171.17, 170.56, 168.85, 164.18, 159.32, 155.59, 150.23, 149.97, 148.37, 139.62, 138.18, 136.86, 136.42, 131.95, 131.67, 131.07, 131.02, 130.68, 130.58, 129.89 (2), 129.62, 129.35 (2), 128.73 (2), 127.93 (2), 112.71, 110.89, 106.86, 70.95, 70.75, 70.49, 70.05, 70.00, 67.59, 58.92, 57.34, 57.07, 54.29, 43.05, 39.75, 36.48, 35.18, 26.45 (3), 16.03, 14.40, 13.10, 11.78; HRMS (ESI) *m/z*: $[M + Na]^+$ Calcd for $C_{53}H_{60}ClN_9NaO_8S_2$ 1072.3593; Found 1072.3563.

1,4D-EG2-MZ1 (**2c**): purified by silica gel column chromatography (1–5% MeOH/$CHCl_3$) followed by PTLC (5% MeOH/$CHCl_3$); Yield 66% from **8c**; ^1H NMR (600 MHz, $CDCl_3$) δ 8.99 (1H, s), 8.68 (1H, s), 7.40 (2H, d, *J* = 9.0 Hz), 7.40–7.44 (1H, m), 7.38 (1H, d, *J* = 8.4 Hz), 7.25–7.33 (7H, m), 6.82

(2H, brd, *J* = 6.6 Hz), 4.75 (1H, t, *J* = 7.8 Hz), 4.65 (1H, dd, *J* = 6.0, 7.8 Hz), 4.52–4.59 (3H, m), 4.29 (1H, dd, *J* = 5.4 and 15.0 Hz), 4.05–4.15 (3H, m), 3.94 (1H, d, *J* = 15.6 Hz), 3.89 (1H, d, *J* = 15.6 Hz), 3.81 (2H, brt, *J* = 4.6 Hz), 3.58–3.74 (6H, m), 3.47 (1H, dd, *J* = 5.4, 7.8 Hz), 2.66 (3H, s), 2.49 (3H, s), 2.46–2.52 (1H, m), 2.38 (3H, s), 2.10-2.15 (1H, m), 1.78-1.92 (3H, brs), 1.70 (3H, s), 0.96 (9H, s); $^{13}C\{^{1}H\}$ NMR (150 MHz, $CDCl_3$) δ 171.26, 170.85, 170.26, 168.48, 164.16, 155.58, 155.27, 150.33, 149.97, 148.39, 138.15, 136.91, 136.42, 131.97, 131.74, 131.63, 131.07, 130.94, 130.81, 130.50, 129.85 (2), 129.44 (2), 128.75(2), 128.08 (2), 121.45 (2), 115.20 (2), 71.13, 70.53, 70.27, 70.08, 69.93, 67.78, 58.55, 57.05, 56.86, 54.60, 43.16, 40.17, 35.99, 35.11, 26.37 (3), 16.01, 14.37, 13.09, 11.77; HRMS (ESI) *m*/*z*: $[M + Na]^+$ Calcd for $C_{53}H_{60}ClN_9NaO_8S_2$ 1072.3593; Found 1072.3597.

1,2D-EG1-MZ1 (**3a**): purified by silica gel column chromatography (1–5% MeOH/$CHCl_3$); Yield 90% from **13a**; ^{1}H NMR (400 MHz, $CDCl_3$) δ 9.17 (1H, s), 8.68 (1H, s), 7.97 (1H, dd, *J* = 7.8, 1.4 Hz), 7.65 (1H, t, *J* = 6.4 Hz), 7.44 (1H, d, *J* = 9.4 Hz), 7.36 (2H, d, *J* = 8.9 Hz), 7.26–7.17 (5H, m), 7.07–7.01 (1H, m), 7.04 (1H, ddd, *J* = 8.4, 7.4, 1.6 Hz), 6.98–6.91 (2H, m), 4.76 (1H, t, *J* = 8.0 Hz), 4.72–4.66 (2H, m), 4.49 (1H, s), 4.42 (1H, dd, *J* = 15.4, 6.5 Hz), 4.29–4.24 (1H, m), 4.18 (1H, d, *J* = 15.6 Hz), 4.09 (1H, d, *J* = 15.6 Hz), 4.12–4.05 (4H, m), 3.98–3.92 (2H, m), 3.84 (1H, dd, *J* = 15.4, 9.2 Hz), 3.70–3.63 (1H, m), 3.67 (1H, dd, *J* = 15.2, 4.7 Hz), 3.35–2.90 (2H, br s), 2.63 (3H, s), 2.45 (3H, s), 2.39 (3H, s), 2.28 (1H, ddd, *J* = 13.3, 8.4, 4.5 Hz), 2.14 (1H, dd, *J* = 13.3, 7.9 Hz), 1.64 (3H,s), 0.92 (3H, s); $^{13}C\{^{1}H\}$ NMR (100 MHz, $CDCl_3$) δ 171.56, 170.96, 169.97, 169.25, 164.14, 155..61,

150.17, 149.93, 149.27, 148.07, 138.28, 136.86, 136.39, 131.88, 131.80, 131.11, 131.07,130.67, 130.25, 129.99 (2), 129.17, 128.68 (2), 129.68 (2), 128.15, 127.62 (2), 124.94, 123.53, 121.96, 113.79, 70.36, 70.20, 70.09, 69.33, 58.86, 57.11, 56.82, 54.09, 42.79, 38.71, 36.90, 35.58, 26.29 (3), 15.92, 14.37, 13.09, 11.74; HRMS (ESI) *m*/*z*: $[M + Na]^+$ Calcd for $C_{51}H_{56}ClN_{9Na}O_7S_2Na$ 1028.3310; Found 1028.3330.

1,3D-EG1-MZ1 (**3b**): purified by silica gel column chromatography (1–5% MeOH/$CHCl_3$); Yield 59% from **13b**; ^1H NMR (400 MHz, $CDCl_3$) δ 9.33 (1H, s), 8.62 (1H, s), 7.80 (1H, d, *J* = 5.8 Hz), 7.26–7.17 (12H, m), 7.06 (1H, t, *J* = 7.8 Hz), 6.56 (1H, dd, *J* = 8.0, 1.8 Hz), 4.72 (1H, t, *J* = 8.0 Hz), 4.61 (1H, t, *J* = 6.8 Hz), 4.54 (1H, d, *J* = 9.1 Hz), 4.47 (1H, s), 4.42 (1H, dd, *J* = 15.2, 6.5 Hz), 4.25 (1H, dd, *J* = 15.2, 5.5 Hz), 4.08–3.88 (5H, m), 3.80–3.71 (3H, m), 3.41 (1H, dd, *J* = 14.8, 6.2 Hz), 2.54 (3H, s), 2.38 (3H, s), 2.32 (3H, s), 2.35–2.21 (1H, m), 2.15 (1H, dd, *J* = 13.1, 8.0 Hz), 1.60 (3H, s), 0.90 (9H, s); $^{13}C\{^1H\}$ NMR (100 MHz, $CDCl_3$) δ 171.34, 170.79, 170.06, 168.89, 164.02, 158.90, 155.61, 150.35, 148.08, 139.51, 138.35, 136.88, 136.33, 131.78, 131.14, 130.97, 130.58, 130.41, 129.86 (2), 129.59, 129.40, 129.35, 129.26 (2), 128.70 (2), 127.92 (2), 113.23, 110.79, 107.13, 70.42, 70.36, 70.15, 67.51, 58.78, 56.98, 56.94, 54.25, 43.00, 39.82, 36.75, 35.56, 29.65, 26.39 (3), 15.88, 14.38, 13.08, 11.70; HRMS (ESI) *m*/*z*: $[M + H]^+$ Calcd for $C_{51}H_{56}ClN_9O_7S_2$ 1006.3511; Found 1006.3538.

1,4D-EG1-MZ1 (**3c**): purified by silica gel column chromatography (1–5% MeOH/$CHCl_3$); Yield 34%

from **13c**; ^{1}H NMR (400 MHz, $CDCl_3$) δ 9.20 (1H, s), 8.75 (1H, s), 7.65–7.60 (1H, m), 7.50–7.42 (2H, m), 7.35–7.31 (4H, m), 7.31–7.22 (6H, m), 6.73 (2H, d, *J* = 8.9 Hz), 4.68–4.60 (1H, m), 4.54–4.42 (2H, m), 4.28–4.19 (2H, m), 4.07–3.96 (3H, m), 3.98 (1H, d, *J* = 15.3 Hz), 3.90 (1H, d, *J* = 15.3 Hz), 3.82–3.68 (2H, m), 3.73 (1H, dd, *J* = 14.6, 8.8 Hz), 3.61–3.52 (2H, m), 3.41 (1H, dd, *J* = 14.6, 5.5 Hz), 2.59 (3H, s), 2.41 (3H, s), 2.33 (3H, s), 2.28–2.21 (1H, m), 2.07 (1H, dd, *J* = 13.1, 9.6 Hz), 1.18 (3H, s), 0.88 (9H, s); ^{13}C{^{1}H} NMR (150 MHz, $CDCl_3$) δ 171.09, 170.99, 170.02, 168.53, 164.34, 155.52, 155.05, 150.89, 150.05, 138.59, 137.08, 136.20, 132.18 (2), 131.93, 131.31, 131.01 (2), 130.51, 129.94 (2), 129.39 (2), 128.79 (2), 128.19 (2), 121.52, 115.04, 70.56, 70.44, 70.12, 67.73, 58.66, 57.00, 56.84, 54.55, 43.13, 39.92, 36.16, 45.56, 26.42 (3), 15.61, 14.39, 13.13, 11.78; HRMS (ESI) *m*/*z*: [M + Na]$^{+}$ Calcd for $C_{51}H_{56}ClN_9NaO_7S_2$; Found 1028.3351.

1,2,3T-EG2-MZ1 (**15a**): purified by silica gel column chromatography (2.5–5% MeOH/$CHCl_3$) followed by HPLC (retention time: 12.36 min); Yield 23% from **20a**; ^{1}H NMR (600 MHz, $CDCl_3$) δ 8.71 (1H, s), 8.66 (1H, s), 7.55 (1H, t, *J* = 6.2 Hz), 7.47 (1H, d, *J* = 9.0 Hz), 7.42 (2H, d, *J* = 9.0 Hz), 7.26–7.29 (6H, m), 7.05 (1H, t, *J* = 8.2 Hz), 6.57 (1H, d, *J* = 8.4 Hz), 6.42 (1H, d, *J* = 8.4 Hz), 4.83 (1H, t, *J* = 7.9 Hz), 4.74 (1H, dd, *J* = 5.4, 8.4 Hz), 4.68 (1H, d, *J* = 9.6 Hz), 4.50 (2H, dd, *J* = 3.6, 9.0 Hz), 4.60 (1H, d, *J* = 16.2 Hz), 4.43 (1H, d, *J* = 16.2 Hz) 4.30 (1H, dd, *J* = 15.1, 5.2 Hz), 4.11–4.19 (4H, m), 3.78-3.87 (3H, m), 3.64–3.73 (6H, m), 3.55 (1H, dd, *J* = 15.5, 5.2 Hz), 2.62 (3H, s), 2.49 (3H, s), 2.37 (3H, s), 2.29–2.34 (1H, m), 2.14–2.27 (2H, m), 1.61 (3H, s), 1.44 (9H, s), 0.94 (9H, s); ^{13}C{^{1}H}

NMR (150 MHz, $CDCl_3$) δ 171.50, 171.17, 170.58, 169.66, 168.34, 163.81, 155.77, 155.19, 154.68, 150.12, 149.72, 148.28, 138.45, 136.65, 136.58, 132.05, 131.78, 130.97, 130.71, 130.66, 130.40, 130.06 (2), 129.24 (2), 128.61 (2), 127.76 (2), 127.53, 116.26, 106.81, 82.33, 70.85, 70.49, 70.38, 70.14, 69.32, 68.42, 67.16, 59.01, 56.97, 56.84, 54.08, 42.96, 37.67, 36.69, 35.68, 29.67, 28.03 (3), 26.39 (3), 16.04, 14.31, 13.05, 11.74; HRMS (ESI) *m/z*: $[M + H]^+$ Calcd for $C_{59}H_{71}ClN_9O_{11}S_2$ 1180.4403; Found 1180.4423.

1,2,4T-EG2-MZ1 (**15b**): purified by HPLC (retention time: 17.29 min); Yield 53% from **20b**; ^1H NMR (600 MHz, $CDCl_3$) δ 8.92 (1H, s), 8.66 (1H, s), 8.09 (1H, d, *J* = 3.1 Hz), 7.37–7.39 (3H, m), 7.28–7.33 (7H, m), 6.82 (1H, d, *J* = 8.9 Hz), 6.57 (1H, dd, *J* = 8.9, 3.1 Hz), 4.69 (2H, q, *J* = 7.1 Hz), 4.57 (1H, d, *J* = 8.9 Hz), 4.50 (1H, dd, *J* = 6.0, 15.0 Hz), 4.47 (1H, brs), 4.44 (2H, s), 4.28 (1H, dd, *J* = 15.1, 5.5 Hz), 4.18-4.21 (1H, m), 4.12–4.15 (1H, m), 4.08 (1H, d, *J* = 15.6 Hz), 4.04 (1H, d, *J* = 15.6 Hz), 4.03–4.08 (1H, m), 3.83–3.88 (2H, m), 3.74–3.77 (2H, m), 3.71–3.73 (2H, m), 3.62 (2H, d, *J* = 6.6 Hz), 3.59 (1H, dd, *J* =3.6, 11.4 Hz), 2.64 (3H, s), 2.50 (3H, s), 2.41–2.44 (1H, m), 2.40 (3H, s), 2.08 (1H, dd, *J* = 13.4, 8.2 Hz), 1.66 (3H, s), 1.46 (9H, s), 0.94 (9H, s); $^{13}C\{^1H\}$ NMR (150 MHz, $CDCl_3$) δ 171.21, 170.97, 170.39, 169.01, 168.14, 163.97, 155.58, 152.67, 150.21, 149.91, 148.37, 142.05, 138.26, 136.76, 136.56, 131.98, 131.65, 131.03, 130.86, 130.71, 130.56, 129.94 (2), 129.74, 129.38 (2), 128.65 (2), 128.01 (2), 114.32, 109.86, 107.19, 82.13, 70.94, 70.62, 70.36, 70.09, 69.68, 69.58, 66.24, 58.51, 56.97, 56.80, 54.07, 43.09, 39.95, 36.14, 35.32, 28.03 (3), 26.37 (3), 16.04, 14.42, 13.09,

11.76; HRMS (ESI) *m*/*z*: $[M + Na]^+$ Calcd for $C_{59}H_{70}ClN_9NaO_{11}S_2$ 1202.4222; Found 1202.4215.

1,2,5T-EG2-MZ1 (**15c**): purified by silica gel column chromatography (1–4% MeOH/$CHCl_3$) followed by PTLC (5% MeOH/$CHCl_3$); Yield 57% from **20c**; ^{1}H NMR (600 MHz, $CDCl_3$) δ 8.67 (2H, s), 8.11 (1H, d, *J* = 8.9 Hz), 7.39 (2H, d, *J* = 8.2 Hz), 7.29–7.33 (7H, m), 6.62 (1H, d, *J* = 2.4 Hz), 6.37 (1H, dd, *J* = 8.8, 2.2 Hz), 4.68–4.73 (2H, m), 4.60 (1H, d, *J* = 8.9 Hz), 4.47–4.53 (2H, m), 4.40–4.43 (2H, m), 4.25–4.30 (2H, m), 4.12–4.17 (1H, m), 4.05–4.10 (3H, m), 3.89 (2H, t, *J* = 4.6 Hz), 3.70–3.79 (5H, m), 3.57–3.64 (3H, m), 2.66 (3H, s), 2.51 (3H, s), 2.45 (1H, brs), 2.40 (3H, s), 2.11 (1H, m), 1.80 (1H, brs), 1.66 (3H, s), 1.48 (9H, s), 0.95 (9H, s); ^{13}C{^{1}H} NMR (150 MHz, $CDCl_3$) δ 171.05, 170.32, 168.69, 167.91, 163.86, 155.63, 154.57, 150.22, 149.85, 149.22, 148.34, 138.29, 136.69, 136.56, 131.99, 131.62, 130.96, 130.79, 130.68, 130.51, 129.91 (2), 129.33 (2), 128.63 (2), 128.03 (2), 122.45, 121.65, 104.56, 101.53, 82.42, 70.89 (2), 70.36, 70.10, 69.27, 68.49, 65.81, 58.57, 56.86, 56.74, 54.17, 43.05, 39.79, 38.57, 36.22, 35.46, 28.02 (3), 26.37 (3), 16.03, 14.39, 13.07, 11.77; HRMS (ESI) *m*/*z*: $[M + H]^+$ Calcd for $C_{59}H_{71}ClN_9O_{11}S_2$ 1180.4403; Found 1180.4380.

1,2,6T-EG2-MZ1 (**15d**): purified by silica gel column chromatography (1–5% MeOH/$CHCl_3$) followed by HPLC (retention time: 15.09 min); Yield 33% from **20d**; ^{1}H NMR (600 MHz, $CDCl_3$) δ 9.18 (1H, s), 8.66 (1H, s), 8.03 (1H, d, *J* = 8.2 Hz), 7.47 (1H, d, *J* = 8.9 Hz), 7.43 (1H, t, *J* = 5.5 Hz), 7.38 (2H, d, *J* = 8.2 Hz), 7.32 (2H, d, *J* = 7.9 Hz), 7.25-7.29 (4H, m), 6.98 (1H, t, *J* = 8.2 Hz), 6.51 (1H, d, *J* = 8.2 Hz), 4.70 (1H, dd, *J* = 8.9, 5.2 Hz), 4.65 (1H, t, *J* = 8.1 Hz), 4.56 (1H, d, *J* = 8.9 Hz),

4.51 (2H, s), 4.41–4.47 (3H, m), 4.32 (1H, m), 4.27 (1H, dd, *J* = 15.1, 5.5 Hz), 4.09 (1H, d, *J* = 15.6 Hz), 4.04 (2H, d, *J* = 15.0 Hz), 3.79 (2H, t, *J* = 4.1 Hz), 3.74–3.77 (4H, m), 3.64–3.70 (1H, m), 3.53–3.57 (2H, m), 2.63 (3H, s), 2.50 (3H, s), 2.39 (3H, s), 2.35 (1H, m), 1.94 (1H, dd, *J* = 13.2, 8.1 Hz), 1.65 (3H, s), 1.47 (9H, s), 0.93 (9H, s); $^{13}C\{^{1}H\}$ NMR (150 MHz, $CDCl_3$) δ 171.16, 171.10, 170.61, 169.37, 167.69, 163.97, 155.56, 150.69, 150.16, 150.01, 148.35, 138.41, 136.70, 136.60, 136.41, 133.49, 132.03, 131.72, 131.04, 130.75, 130.60, 130.51, 129.95 (2), 129.34 (2), 128.63 (2), 127.95 (2), 124.08, 113.74, 108.16, 82.48, 72.09, 71.02, 70.35, 70.30, 70.21, 69.97, 65.97, 58.47, 57.05, 56.90, 53.98, 43.00, 39.76, 36.13, 35.27, 28.04 (3), 26.38 (3), 16.04, 14.43, 13.08, 11.74; HRMS (ESI) *m*/*z*: $[M + H]^+$ Calcd for $C_{59}H_{71}ClN_9O_{11}S_2$ 1180.4403; Found 1180.4410.

Cell culture, lysis, and Western blotting

Human HT1080 cells were obtained from ATCC and maintained at 37°C 5% CO_2 in Dulbecco's Modified Eagle's Medium (DMEM) high-glucose medium (Sigma-Aldrich) supplemented with 10% fetal bovine serum (FBS) (Sigma-Aldrich). For Western blotting, cells were lysed in lysis buffer (10 mM Tris-HCl [pH, 7.5], 150 mM NaCl, 0.5 mM EDTA, 1% NP40, 0.5% Triton X-100, 10% glycerol) supplemented with protease inhibitor cocktail (Nacalai Tesque) and then sonicated extensively (Handy Sonic, TOMY Seiko). Soluble lysates were subjected to Western blotting using anti-BRD4 (Cell Signaling Technology, #13440) and anti-β-actin (Santa Cruz Biotechnology, #47778) antibodies.

Chemiluminescence signals were detected on a FUSION imaging system (Vilber-Lourmat). Bands were quantified using an Evolution-Capt EDGE imaging system (Vilber-Lourmat). Half-life of BRD4 (Fig. 4) was calculated from the band intensities of anti-BRD4 blots (0 to 120 min treatment of either MZ1 or **15c**).

Supporting Information

Supporting Information is available free of charge at https://pubs.acs.org/doi/XXXXXX.

This information includes Figure S1, general experimental procedures for the synthesis of **8a**-**c**, **13a**-**c**, and **20a**-**d**, synthesis and characterization data of intermediates, and NMR spectra of synthetic compounds (PDF).

Notes

The authors declare no competing financial interest.

References

(1) Toure, M. and Crews, C. M. (2016) Small-molecule PROTACS: New approaches to protein degradation. *Angew Chem Int Ed, 55*, 1966-1973.

(2) Lai, A. C. and Crews, C. M. (2017) Induced protein degradation: An emerging drug discovery paradigm. *Nat Rev Drug Discov, 16*, 101-114.

(3) Bondeson, D. P., Smith, B. E., Burslem, G. M., Buhimschi, A. D., Hines, J., Jaime-Figueroa, S., Wang, J., Hamman, B. D., Ishchenko, A. and Crews, C. M. (2018) Lessons in PROTAC design from selective

degradation with a promiscuous warhead. *Cell Chem Biol, 25*, 78-87.
(4) Nguyen, T. V., Li, J., Lu, C. J., Mamrosh, J. L., Lu, G., Cathers, B. E. and Deshaies, R. J. (2017) p97/VCP promotes degradation of CRBN substrate glutamine synthetase and neosubstrates. *Proc Natl Acad Sci U S A, 114*, 3565-3571.
(5) Kaiho-Soma, A., Akizuki, Y., Igarashi, K., Endo, A., Shoda, T., Kawase, Y., Demizu, Y., Naito, M., Saeki, Y., Tanaka, K. and Ohtake, F. (2021) TRIP12 promotes small-molecule-induced degradation through K29/K48-branched ubiquitin chains. *Mol Cell, 81*, 1411-1424 e1417.
(6) Lu, G., Weng, S., Matyskiela, M., Zheng, X., Fang, W., Wood, S., Surka, C., Mizukoshi, R., Lu, C. C., Mendy, D., Jang, I. S., Wang, K., Marella, M., Couto, S., Cathers, B., Carmichael, J., Chamberlain, P. and Rolfe, M. (2018) UBE2G1 governs the destruction of cereblon neomorphic substrates. *Elife, 7*, e40958.
(7) Mayor-Ruiz, C., Jaeger, M. G., Bauer, S., Brand, M., Sin, C., Hanzl, A., Mueller, A. C., Menche, J. and Winter, G. E. (2019) Plasticity of the Cullin-RING ligase repertoire shapes sensitivity to ligand-induced Pprotein degradation. *Mol Cell, 75*, 849-858.
(8) Kaji, T., Koga, H., Kuroha, M., Akimoto, T. and Hayata, K. (2020) Characterization of cereblon-dependent targeted protein degrader by visualizing the spatiotemporal ternary complex formation in cells. *Sci Rep, 10*, 3088.
(9) Chung, C. I., Zhang, Q. and Shu, X. (2018) Dynamic imaging of small molecule induced protein-protein interactions in living cells with a fluorophore phase transition based approach. *Anal Chem, 90*, 14287-14293.
(10) Cyrus, K., Wehenkel, M., Choi, E. Y., Swanson, H. and Kim, K. B. (2010) Two-headed PROTAC: an effective new tool for targeted protein degradation. *Chembiochem, 11*, 1531-1534.
(11) Imaide, S., Riching, K. M., Vetma, V., Whitworth, C., Hughes, S. J., Trainor, N., Mahan, S. D., Muphy, N., Chan, K.-H., Testa, A., Maniaci, C., Urh, M., Daniels, D. L. and Ciulli, A. (2020) Trivalent PROTACs enhaunce protein degradation through cooperativity and avidity. *ChemRxiv*, 10.26434/chemrxiv.13218695.v13218691.
(12) Zengerle, M., Chan, K. H. and Ciulli, A. (2015) Selective small molecule induced degradation of the BET bromodomain protein BRD4. *ACS Chem Biol, 10*, 1770-1777.
(13) Gadd, M. S., Testa, A., Lucas, X., Chan, K. H., Chen, W., Lamont, D. J., Zengerle, M. and Ciulli, A. (2017) Structural basis of PROTAC cooperative recognition for selective protein degradation. *Nat Chem Biol, 13*, 514-521.
(14) Tanaka, M., Roberts, J. M., Seo, H. S., Souza, A., Paulk, J., Scott, T. G., DeAngelo, S. L., Dhe-Paganon, S. and Bradner, J. E. (2016) Design and characterization of bivalent BET inhibitors. *Nat Chem Biol, 12*, 1089-1096.
(15) Dragovich, P. S., Pillow, T. H., Blake, R. A., Sadowsky, J. D., Adaligil, E., Adhikari, P., Bhakta, S., Blaquiere, N., Chen, J., Dela Cruz-Chuh, J., Gascoigne, K. E., Hartman, S. J., He, M., Kaufman, S., Kleinheinz, T., Kozak, K. R., Liu, L., Liu, L., Liu, Q., Lu, Y., Meng, F., Mulvihill, M. M., O'Donohue, A.,

Rowntree, R. K., Staben, L. R., Staben, S. T., Wai, J., Wang, J., Wei, B., Wilson, C., Xin, J., Xu, Z., Yao, H., Zhang, D., Zhang, H., Zhou, H. and Zhu, X. (2021) Antibody-mediated delivery of chimeric BRD4 degraders. Part 1: Exploration of antibody linker, payload loading, and payload molecular properties. *J Med Chem, 64*, 2534-2575.

(16) Dragovich, P. S., Pillow, T. H., Blake, R. A., Sadowsky, J. D., Adaligil, E., Adhikari, P., Chen, J., Corr, N., Dela Cruz-Chuh, J., Del Rosario, G., Fullerton, A., Hartman, S. J., Jiang, F., Kaufman, S., Kleinheinz, T., Kozak, K. R., Liu, L., Lu, Y., Mulvihill, M. M., Murray, J. M., O'Donohue, A., Rowntree, R. K., Sawyer, W. S., Staben, L. R., Wai, J., Wang, J., Wei, B., Wei, W., Xu, Z., Yao, H., Yu, S. F., Zhang, D., Zhang, H., Zhang, S., Zhao, Y., Zhou, H. and Zhu, X. (2021) Antibody-mediated delivery of chimeric BRD4 degraders. Part 2: Improvement of in vitro antiproliferation activity and in vivo antitumor efficacy. *J Med Chem, 64*, 2576-2607.

(17) Liu, J., Chen, H., Liu, Y., Shen, Y., Meng, F., Kaniskan, H. U., Jin, J. and Wei, W. (2021) Cancer selective target degradation by folate-caged PROTACs. *J Am Chem Soc, 143*, 7380-7387.

(18) Yamaguchi, T., Asanuma, M., Nakanishi, S., Saito, Y., Okazaki, M., Dodo, K. and Sodeoka, M. (2014) Turn-ON fluorescent affinity labeliing using a small bifunctional *O*-nitrobenzodiazole unit. *Chem Sci, 5*, 1021-1029.

(19) Tsukiji, S., Miyagawa, M., Takaoka, Y., Tamura, T. and Hamachi, I. (2009) Ligand-directed tosyl chemistry for protein labeling in vivo. *Nat Chem Biol, 5*, 341-343.

(20) Qian, Y., Dong, H., Wang, J., Berlin, M., Siu, K., Crew, A. P. and Crews, C. M. (2017) Preparation of bifunctional PROTAC compounds and methods for the enhanced degradation of targeted bromodomain-containing proteins. *WO2017030814 A1*.

(21) Buckley, D. L., Raina, K., Darricarrere, N., Hines, J., Gustafson, J. L., Smith, I. E., Miah, A. H., Harling, J. D. and Crews, C. M. (2015) HaloPROTACS: Use of small molecule PROTACs to induce degradation of Halo tag fusion proteins. *ACS Chem Biol, 10*, 1831-1837.

(22) Carpino, L. A., Imazumi, H., El-Faham, A., Ferrer, F. J., Zhang, C., Lee, Y., Foxman, B. M., Henklein, P., Hanay, C., Mugge, C., Wenschuh, H., Klose, J., Beyermann, M. and Bienert, M. (2002) The uronium/guanidinium peptide coupling reagents: finally the true uronium salts. *Angew Chem Int Ed, 41*, 441-445.

(23) Shibuya, M., Sato, T., Tomizawa, M. and Iwabuchi, Y. (2009) Oxoammonium salt/NaClO2: an expedient, catalytic system for one-pot oxidation of primary alcohols to carboxylic acids with broad substrate applicability. *Chem Commun*, 1739-1741.

(24) El-Faham, A., Subiros Funosas, R., Prohens, R. and Albericio, F. (2009) COMU: a safer and more effective replacement for benzotriazole-based uronium coupling reagents. *Chem Eur J, 15*, 9404-9416.